

Low-Cost Doppler Radar Structural Monitoring

Subjects: Engineering, Biomedical

Contributor: Changzhi Li

Low-Cost Microwave Doppler Radar Systems is an alternative noncontact solution for structural condition monitoring. In addition, by leveraging their capability of providing the target velocity information, the radar-based remote monitoring of complex rotating structures can also be accomplished. Modern radar systems are compact, able to be easily integrated in sensor networks, and can deliver high accuracy measurements.

Keywords: Doppler radar ; displacement measurement ; low-cost radar ; micro-Doppler ; portable radar ; remote sensing ; radar network

1. Introduction

Radars have been employed since 1940s ^[1]. In the past, they were mainly used in military, navigation, and meteorology due to high costs and bulky sizes. Thanks to the fast and significant advancements in the semiconductor industry, radars are being miniaturized and assembled on printed circuit boards (PCB) or even integrated into a single chip with antenna-on-chip/antenna-in-package technologies ^{[2][3][4][5]}. In the last decades, portable short-range radars have been investigated for human and animal vital signs, remote voice recording, gait analysis, fall detection, gesture characterization, occupancy sensing, and security applications ^{[6][7][8][9][10][11][12][13][14][15][16][17][18][19]}. Biomedical Doppler radars have also been employed in cancer radiotherapy for respiratory gating and tumor tracking for motion-adaptive radiotherapy ^{[20][21][22]}. In addition, short-range radars can be used to provide time-frequency analysis of microwave signals backscattered by rotating structures such as wind turbines ^{[23][24][25][26][27][28]}.

Structural health monitoring (SHM) is the process of continuous observation of a structure or mechanical system using one or multiple sensors to provide information about its true capacity, which is altered by age and/or accidental damage. By sensing low-frequency small-amplitude mechanical vibration or deflection of structures, radars may also be successfully employed for the SHM of infrastructures. As the aging of worldwide infrastructures raises concerns and the appearance of new structures forces researchers and engineers to look for alternative solutions for SHM measurements and the improvement of existing ones, private industries and government organizations demand technologies that are able to detect structural damage at the earliest possible time to avoid life-threatening situations and economical losses.

Several technologies targeting SHM have been proposed in the past decades. Accelerometers are commonly used to evaluate the infrastructure health condition and to extract damage-sensitive features because they are relatively cost-effective and can be readily instrumented. Nevertheless, the double integration of the acceleration data makes displacement measurements susceptible to integral drift errors ^[29]. Strain sensors, laser displacement sensors, and vision-based systems are also representatives of nonintrusive solutions for SHM applications. However, these sensors present practical limitations. The measurements retrieved by strain gauges are sensitive to temperature variations, and they may need periodical calibration. Laser displacement sensors are sensitive to the measurement range and the structure's surface condition. Vision-based systems demand large data storage, high computational load for image recognition and are not robust against ambient light.

On the other hand, radars can make use of different types of waveforms for the targeted application. Continuous-wave (CW) radars have simple architecture, allowing for easier integration and lower power consumption, which makes them appealing for portable applications. In a basic CW radar system, the radio frequency (RF) wave is radiated, and an echo returns after being backscattered by a surrounding target. If the target is moving, a shift in the received radar signal due to the Doppler effect is observed. The target's range can only be assessed by modulated CW radars. Modulated CW radars such as frequency-modulated continuous-wave (FMCW) radars and stepped-frequency continuous-wave (SFCW) radars are popular candidates for applications that require range and/or Doppler information. In contrast, unmodulated CW radars, widely known as Doppler radars, do not have range discrimination capability. Nonetheless, Doppler radars can measure time-varying small-amplitude periodical motion with high accuracy ^[2].

The most common radars employed on structural condition monitoring are the ground-based interferometric (GBI) radars. Their use for SHM applications has a relatively long history. The inspiration for the utilization of GBI radars on the monitoring of structures such as building or bridges came from the success of spaceborne synthetic aperture radar (SAR) radar systems, which operate at high orbits and detect ground changes based on the phase information of radar images [30][31]. During onsite testing, these sensors are typically mounted on a tripod and pointed towards bridges, landslides, towers, and dams [32][33][34][35][36][37][38][39][40][41][42][43][44][45][46][47][48][49][50][51][52][53][54][55]. The main difference between GBIR and other portable radar sensors is their relatively large detection range due to the use of bulky, high directivity antennas and waveguide-based components [38]. By transmitting and receiving electromagnetic waves at microwave frequencies, they can remotely detect small displacements of targets using the interferometric technique, and they are also able to distinguish the real displacement of targets of interest from clutter since the vast majority of GBI radar systems employs stepped-frequency continuous-wave (SFCW) or frequency-modulated continuous-wave (FMCW) radar sensors. These systems can operate without any angular resolution or with angular resolution obtained through the rotation of the radar or the movement of the radar along a linear mechanical guide. GBI radars are powerful tools on the estimation of vibration parameters of structures with large areas (bridges, mines, buildings). Bridge monitoring using portable GBI radars dates back to the 2000s [32]. The evaluation of the bridge displacement along the radial direction by an SFCW or FMCW radar systems starts by choosing the range bin associated with different parts of the structure. After the selection of the range bin, the displacement of the target is recovered by demodulating the phase variations of the received signal during the detection time. Another important parameter of modulated wave radar is the range resolution, which is a function of the transmitted bandwidth and is the minimum distance to resolve two or more adjacent targets on the same bearing.

Most monostatic radars detect motion along the radial direction, and the movement of real large targets such as buildings or bridges consists of more than one component. To address the challenge of simultaneously measuring displacements along different directions, the most recent work on SHM based on GBI radars proposed a multi-monostatic 17.2-GHz FMCW radar for the remote monitoring of bridges [55]. They employed two different interferometric radars placed at different positions to measure two components of a bridge's deck motion. The used radar system was a modified version of a multiple-input multiple-output (MIMO) GBI radar (IBIS-FM MIMO by IDS Company) that operated with two pairs of transmitting (Tx) and receiving (Rx) antennas (four possible baseband channels). Only two channels were effectively used to retrieve the displacements at two different positions (23 m and 33 m away from the main radar) on the bridge. RF cables were utilized to connect the second pair of Tx/Rx antennas to the main radar system, allowing for the multi-monostatic radar architecture. The radar operated sequentially in a single channel modality, but the time duration between four acquisitions was relatively short (5–12 ms), especially for SHM applications. The cable loss and the time shifts were compensated by low noise amplifiers and by digital signal processing techniques, respectively. The authors chose the 127-m long Varlungo Bridge in Firenze, Italy, to conduct the full-scale experiments. The vehicular traffic provoked the bridge vibration, but a significant change on the displacement was only observed when a truck moved on the bridge. With this strategy, the authors were able to retrieve the displacement vector (y - z plane) and the natural frequencies for the two different radar targets. However, no discussion was made towards modal analysis measurements. In addition, the proposed method relies on choosing an appropriated distance between the main radar and the second pair of Tx/Rx antennas, which must be large enough to allow the evaluation of the vector displacement using the two motion components. The radar had achieved submillimeter accuracy during measurements in a controlled environment with an oscillating corner reflector placed 12.88 m away from the main radar and 7.33 m away from the second pair of antennas. Seismic accelerometer measurements (PCB 393B31 by PCB piezotronics) provided the ground truth.

2. Low-Cost Doppler Radars for Structural Health Monitoring

Doppler radars emit a single-tone microwave signal of frequency f_t . The reflected radio-frequency signal is frequency/phase-modulated due to the Doppler effect assuming that the target is moving. The microwave frequency associated with the translational speed v of a point-scatterer target is calculated as $f_r = f_t(1+v/c)/(1-v/c)$, and can be easily retrieved by spectral analysis. If the target consists of several moving parts, the contributions of various point-scatterers produce micro-Doppler signatures, which can be exploited for the extraction of other parameters not related to the main target's movement [23]. For example, when one does hand gestures in front of a radar sensor, not only will the Doppler frequencies associated with the hand's movement be captured, but also the frequencies associated with the movements of other parts of the human body such as the arm and the elbow [17][18].

Assuming that a simple homodyne Doppler radar illuminates a structure comprised of rotating blades, as seen in Figure 1, the reflected signal is phase-modulated by their movement. The returned echoes are mixed with the same transmitted signal by a quadrature-mixer to generate in-phase ($I(t)$) and quadrature-phase ($Q(t)$) baseband responses. The analytic form of the amplitude-normalized baseband signal can be cast as $s_b(t) = I(t) + jQ(t) = \sum_{k=1}^K \exp(-j4\pi R_k(t)/\lambda)$, where the time-

varying distances between the radar sensor and each of the K scatterers are $R_k(t)$ and K is the number of scatterers. Taking into account that the blade's surface backscatters significant radar signals in the perpendicular direction, the distance between each scatterer and the radar makes the total received signals be coherently added. Therefore, its micro-Doppler signatures will have the form of flashes in the time-Doppler maps [28].

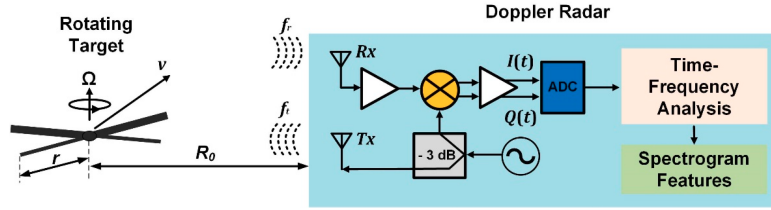


Figure 1. Block diagram for structural health monitoring (SHM) based on low-cost Doppler radars using time-frequency analysis of micro-Doppler signatures.

However, unique signatures with sinusoidal forms, called halos, are also observed in the spectrograms for rotating structures with translational velocity equals to zero ($v = 0$) [28]. The blade tips should be considered as point-scatterer targets. Considering that R_0 is the nominal distance between the radar and the rotation center, r is the blade radius, and Ω is the angular velocity, the distance between the blade tips can be modeled as $R_{tip} = R_0 + r\sin(\Omega t)$. For simplicity, the initial rotation angle on the rotation plane was suppressed. By applying the first derivative to the phase history of the complex baseband signal $s_{tip}(t) =$

$$= -2$$

$f_D(t) = -2r\Omega\cos(\Omega t)/\lambda$, which demonstrates that the micro-Doppler signatures of the blade tips are theoretically sinusoidal. In fact, they appear as quasi-sinusoidal signatures in the time-Doppler maps due to the short-range detection [28].

On the other hand, if the target presents a periodical linear motion, its displacement also provokes the phase-modulation of the previously transmitted radar signal. **Figure 2** illustrates the block diagram for the remote vibration monitoring based on a Doppler radar system. Again, the backscattered reflected signal $R(t)$ is mixed with the same transmitted signal $T(t)$ by a quadrature-mixer to generate in-phase and quadrature-phase baseband responses. After the correct condition of the DC offsets, amplitude normalization, and circle fitting for the recorded I/Q baseband signals, the detected displacement can be estimated by nonlinear phase-demodulation algorithms, which combine both the in-phase and quadrature-phase signals to retrieve the changes in the phase angles of consecutive sampling points. Assume that the structure vibrates with a time-varying displacement $x(t) = m\sin(\omega_0 t)$, where m is the amplitude and the ω_0 is the angular dominant frequency of the periodical motion. The two baseband responses can be written as $I(t) = \sin(4\pi x(t)/\lambda + \theta)$ and $Q(t) = \cos(4\pi x(t)/\lambda + \theta)$, where θ is the sum of the phase shift due to the nominal distance between the radar and the target, as well as the residual phase noise. By using arctangent demodulation, the vibration motion $x(t)$ can be recovered as $x(t) = (\lambda/4\pi) \times \{\arctan[I(t)/Q(t)] - \theta\} = (\lambda/4\pi) \times \{\arctan[\sin(4\pi x(t)/\lambda + \theta)/\cos(4\pi x(t)/\lambda + \theta)] - \theta\}$, where λ is the wavelength of the transmitted RF signal [56]. Since the Doppler radars take advantage of the range correlation effect, the residual phase noise is negligible [57]. θ is only dependent on the constant nominal distance between the target and the radar. Therefore, it can be removed by subtracting the mean value.

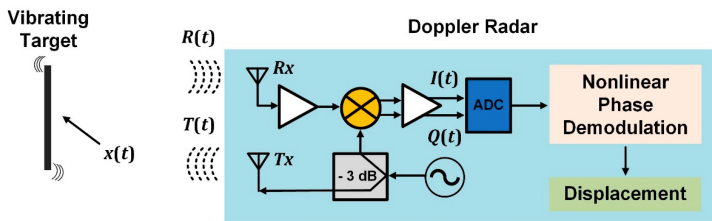


Figure 2. Block diagram for the SHM based on low-

cost Doppler radars through remote vibration monitoring.

Other transceiver architectures such as digital-IF receiver or double-sideband radars can also be utilized. Interested readers are encouraged to refer to [58][59][60] for practical discussions on different Doppler radar architectures.

3. Conclusions

Powered by the advancements of semiconductor technologies, Doppler radar can be miniaturized, which led to vast practical implementations in the civilian world. The recent technical advancements on digital signal processing pushed the technology further into smart integration with embedded systems. In addition, the potential costs of Doppler radar sensors after CMOS integration and mass production would possibly make them even more appealing than other noncontact approaches for SHM such as camera systems and laser vibrometers. Beamforming technology can also be exploited to

address the current issue of measuring only the displacement on the radial direction. Furthermore, by leveraging the compactness of low-cost Doppler radars, radar sensor networks can be deployed. Although the adoption of low-cost, compact radars still lags behind other technologies, SHM researchers and engineers can be optimistic about the promising possibilities for low-cost radars with the rapid dissemination of chipset-based sensors and migration to mm-wave bands.

References

1. Muñoz-Ferreras, J.-M.; Peng, Z.; Tang, Y.; Gómez-García, R.; Liang, D.; Li, C. Short-range Doppler-radar signatures from industrial wind turbines: Theory, simulations, and measurements. *IEEE Trans. Instrum. Meas.* 2016, 65, 2108–2119.
2. Park, B.; Boric-Lubecke, O.; Lubecke, V. Arctangent demodulation with DC offset compensation in quadrature Doppler radar receiver systems. *IEEE Trans. Microw. Theory Tech.* 2007, 55, 10731079.
3. Droitcour, A.D.; Boric-Lubecke, O.; Lubecke, V.M.; Lin, J.; Kovac, G.T. Range correlation and I/Q performance benefits in single-chip silicon Doppler radars for noncontact cardiopulmonary monitoring. *IEEE Trans. Microw. Theory Tech.* 2004, 52, 838–848.
4. Wei, C.; Lin, J. Digitally assisted low IF architecture for noncontact vital sign detection. In *Proceedings of the IEEE MTT-S International Microwave Symposium*, Phoenix, AZ, USA, 17–22 May 2015; pp. 1–4.
5. Gu, C. Short-Range Noncontact Sensors for Healthcare and Other Emerging Applications: A Review. *Sensors* 2016, 16, 1169.
6. Ma, X.; Li, L.; You, X.; Lin, J. Envelope detection for a double-sideband Low IF CW radar. In *Proceedings of the IEEE/MTT-S International Microwave Symposium—IMS*, Philadelphia, PA, USA, 10–15 June 2018; pp. 240–243.
7. Li, C.; Lin, J. Random Body Movement Cancellation in Doppler Radar Vital Sign Detection. *IEEE Trans. Microw. Theory Tech.* 2008, 56, 3143–3152.
8. Xiong, J.; Hong, H.; Zhang, H.; Wang, N.; Chu, H.; Zhu, X. Multitarget Respiration Detection with Adaptive Digital Beamforming Technique Based on SIMO Radar. *IEEE Trans. Microw. Theory Tech.* 2020, 68, 4814–4824.
9. Wang, P.; Ma, Y.; Liang, F.; Zhang, Y.; Yu, X.; Li, Z.; An, Q.; Lv, H.; Wang, J. Non-Contact Vital Signs Monitoring of Dog and Cat Using a UWB Radar. *Animals* 2020, 10, 205.
10. Rodriguez, D.; Li, C. Sensitivity and Distortion Analysis of a 125-GHz Interferometry Radar for Submicrometer Motion Sensing Applications. *IEEE Trans. Microw. Theory Tech.* 2019, 67, 5384–5395.
11. Wang, Y.; Ling, H.; Chen, V.C. ISAR motion compensation via adaptive joint time-frequency technique. *IEEE Trans. Aerosp. Electron. Syst.* 1998, 34, 670–677.
12. Ding, C.; Hong, H.; Zou, Y.; Chu, H.; Zhu, X.; Fioranelli, F.; Le Kernec, J.; Li, C. Continuous Human Motion Recognition with a Dynamic Range-Doppler Trajectory Method Based on FMCW Radar. *IEEE Trans. Geosci. Remote Sens.* 2019, 57, 6821–6831.
13. Ram, S.S.; Ling, H. Through-wall tracking of human movers using joint Doppler and array processing. *IEEE Trans. Geosci. Remote Sens.* 2008, 5, 537–541.
14. Kim, Y.; Ling, H. Human activity classification based on micro-Doppler signatures using an artificial neural network. In *Proceedings of the IEEE Antennas and Propagation Society International Symposium*, San Diego, CA, USA, 5–11 July 2008; pp. 1–4.
15. Kim, Y.; Ling, H. Human activity classification based on micro-Doppler signatures using a support vector machine. *IEEE Trans. Geosci. Remote Sens.* 2009, 47, 1328–1337.
16. Ram, S.S.; Christianson, C.; Kim, Y.; Ling, H. Simulation and analysis of human micro-Dopplers in through-wall environments. *IEEE Trans. Geosci. Remote Sens.* 2010, 48, 2015–2023.
17. Rodrigues, D.V.Q.; Li, C. Hand gesture recognition using FMCW radar in multi-person scenario. In *Proceedings of the IEEE MTT-S Radio and Wireless Symposium (RWS)*, Virtual Conference. 17–20 January 2021.
18. Rodrigues, D.V.Q.; Li, C. Noncontact exercise monitoring in multi-person scenario with frequency-modulated continuous-wave radar. In *Proceedings of the IEEE MTT-S International Microwave Biomedical Conference (IMBioC)*, Virtual Conference. 14–17 December 2020.
19. Li, Y.; Peng, Z.; Pal, R.; Li, C. Potential Active Shooter Detection Based on Radar Micro-Doppler and Range-Doppler Analysis Using Artificial Neural Network. *IEEE Sens. J.* 2019, 19, 1052–1063.

20. Gu, C.; Salmani, Z.; Zhang, H.; Li, C. Antenna array technology for radar respiration measurement in motion-adaptive lung cancer radiotherapy. In Proceedings of the IEEE Topical Conference on Biomedical Wireless Technologies, Networks, and Sensing Systems (BioWireleSS), Santa Clara, CA, USA, 15–18 January 2012; pp. 21–24.
21. Gu, C.; Li, R.; Zhang, H.; Fung, A.Y.C.; Torres, C.; Jiang, S.B.; Li, C. Accurate respiration measurement using DC-coupled continuous-wave radar sensor for motion-adaptive cancer radiotherapy. *IEEE Trans. Biomed. Eng.* 2012, 59, 3117–3123.
22. Klemm, M.; Craddock, I.J.; Leendertz, J.A.; Preece, A.; Benjamin, R. Radar-Based Breast Cancer Detection Using a Hemispherical Antenna Array—Experimental Results. *IEEE Trans. Antennas Propag.* 2009, 57, 1692–1704.
23. Chen, V.C.; Ling, H. *Time-Frequency Transforms for Radar Imaging and Signal Analysis*; Artech House: Norwood, MA, USA, 2002.
24. Li, J.; Ling, H. Application of adaptive chirplet representation for ISAR feature extraction from targets with rotating parts. *IEE Proc. Radar Sonar Navig.* 2003, 150, 284–291.
25. Naqvi, A.; Yang, S.-T.; Ling, H. Investigation of Doppler features from wind turbine scattering. *IEEE Antennas Wireless Propag. Lett.* 2010, 9, 485–488.
26. Li, C.J.; Ling, H. On simulating the high-resolution radar image of a wind turbine. In Proceedings of the 10th European Conference on Antennas and Propagation (EuCAP), Davos, Switzerland, 10–15 April 2016; pp. 1–3.
27. Whiteloni, N.; Yang, S.-T.; Ling, H. Application of nearfield to far-field transformation to Doppler features from wind turbine scattering. *IEEE Trans. Antennas Propag.* 2012, 60, 1660–1665.
28. Muñoz-Ferreras, J.-M.; Peng, Z.; Tang, Y.; Gómez-García, R.; Liang, D.; Li, C. Short-range Doppler-radar signatures from industrial wind turbines: Theory, simulations, and measurements. *IEEE Trans. Instrum. Meas.* 2016, 65, 2108–2119.
29. Thenozhi, S.; Yu, W.; Garrido, R. A novel numerical integrator for structural health monitoring. In Proceedings of the 5th International Symposium on Resilient Control Systems, Salt Lake City, UT, USA, 14–16 August 2012; pp. 92–97.
30. Srivastava, S.K.; Lukowski, T.I.; Gray, R.B.; Shepherd, N.W.; Hawkins, R.K. RADARSAT: Image quality management and performance results. In Proceedings of the Canadian Conference on Electrical and Computer Engineering, Calgary, AB, Canada, 26–29 May 1996; Volume 1, pp. 21–23.
31. Farrar, C.R.; Darling, T.W.; Migliori, A.; Baker, W.E.; Adams, M. Microwave interferometers for non-contact vibration measurements on large structures. *Mech. Syst. Signal Process.* 1999, 13, 241–253.
32. Pieraccini, M.; Tarchi, D.; Rudolf, H.; Leva, D.; Luzi, G.; Bartoli, G.; Atzeni, C. Structural static testing by interferometric synthetic radar. *NDT E Int.* 2000, 33, 565–570.
33. Tarchi, D.; Casagli, N.; Fanti, R.; Leva, D.D.; Luzi, G.; Pasuto, A.; Pieraccini, M.; Silvano, S. Landslide monitoring by using ground-based SAR interferometry: An example of application to the Tessina landslide in Italy. *Eng. Geol.* 2003, 68, 15–30.
34. Atzeni, C.; Bicci, A.; Dei, D.; Fratini, M.; Pieraccini, M. Remote survey of the Leaning Tower of Pisa by Interferometric Sensing. *IEEE Geosci. Remote Sens. Lett.* 2010, 7, 185–189.
35. Pieraccini, M.; Papi, F.; Donati, N. I-Q imbalance correction of microwave displacement sensors. *Electron. Lett.* 2015, 51, 1021–1023.
36. Luzi, G.; Crosetto, M.; Fernández, E. Radar interferometry for monitoring the vibration characteristics of buildings and civil structures: Recent case studies in Spain. *Sensors* 2017, 17, 669.
37. Di Pasquale, A.; Nico, G.; Pitullo, A.; Prezioso, G. Monitoring Strategies of Earth Dams by Ground-Based Radar Interferometry: How to Extract Useful Information for Seismic Risk Assessment. *Sensors* 2018, 18, 244.
38. Hu, J.; Guo, J.; Xu, Y.; Zhou, L.; Zhang, S.; Fan, K. Differential Ground-Based Radar Interferometry for Slope and Civil Structures Monitoring: Two Case Studies of Landslide and Bridge. *Remote Sens.* 2019, 11, 2887.
39. Moll, J.; Bechtel, K.; Hils, B.; Krozer, V. Mechanical Vibration Sensing for Structural Health Monitoring Using a Millimeter-Wave Doppler Radar Sensor. In Proceedings of the 7th European Workshop on Structural Health Monitoring (EWSHM), Nantes, France, 8–11 July 2014; pp. 1802–1808.
40. Diaferio, M.; Fraddosio, A.; Daniele Piccioni, M.; Castellano, A.; Mangialardi, L.; Soria, L. Some issues in the structural health monitoring of a railway viaduct by ground-based radar interferometry. In Proceedings of the IEEE Workshop on Environmental, Energy, and Structural Monitoring Systems (EESMS), Milan, Italy, 24–25 July 2017; pp. 1–6.
41. Pieraccini, M.; Betti, M.; Forcellini, D.; Dei, D.; Papi, F.; Bartoli, G.; Facchini, L.; Corazzi, R.; Cerisano Kovacevic, V. Radar detection of pedestrian-induced vibrations on Michelangelo's David. *PLoS ONE* 2017, 12, e0174480.

42. Luzi, G.; Crosetto, M.; Angelats, E.; Fernández, E. An interferometric radar sensor for monitoring the vibrations of structures at short. In *MATEC Web of Conferences*; EDP Sciences: Les Ulis, France, 2018; Volume 148, p. 01005.
43. Viviani, F.; Michelini, A.; Mayer, L.; Conni, F. IBIS-ArcSAR: An Innovative Ground-Based SAR System for Slope Monitoring. In *Proceedings of the IGARSS—IEEE International Geoscience and Remote Sensing Symposium*, Valencia, Spain, 22–27 July 2018; pp. 1348–1351.
44. Liu, X.; Li, S.; Tong, X. Two-Level W-ESMD Denoising for Dynamic Deflection Measurement of Railway Bridges by Microwave Interferometry. *IEEE J. Sel. Top. Signal Process.* 2018, 11, 4874–4883.
45. Miccinesi, L.; Pieraccini, M. Monostatic/Bistatic Interferometric Radar for Monitoring Slander Structures. In *Proceedings of the IEEE Conference on Antenna Measurements & Applications (CAMA)*, Kuta, Bali, Indonesia, 23–25 October 2019; pp. 1–4.
46. Castagnetti, C.; Bassoli, E.; Vincenzi, L.; Mancini, F. Dynamic Assessment of Masonry Towers Based on Terrestrial Radar Interferometer and Accelerometers. *Sensors* 2019, 19, 1319.
47. Pieraccini, M.; Miccinesi, L. Ground-Based Radar Interferometry: A Bibliographic Review. *Remote Sens.* 2019, 11, 1029.
48. Pieraccini, M.; Miccinesi, L. An Interferometric MIMO Radar for Bridge Monitoring. *IEEE Geosci. Remote Sens. Lett.* 2019, 16, 1383–1387.
49. Pieraccini, M.; Miccinesi, L.; Abdorazzagh Nejad, A.; Naderi Nejad Fard, A. Experimental Dynamic Impact Factor Assessment of Railway Bridges through a Radar Interferometer. *Remote Sens.* 2019, 11, 2207.
50. Wang, Y.; Dai, K.; Xu, Y.; Zhu, W.; Lu, W.; Shi, Y.; Mei, Z.; Xue, S.; Faulkner, K. Field Testing of Wind Turbine Towers with Contact and Noncontact Vibration Measurement Methods. *J. Perform. Constr. Facil.* 2020, 34, 04019094.
51. Nico, G.; Prezioso, G.; Masci, O.; Artese, S. Dynamic Modal Identification of Telecommunication Towers Using Ground Based Radar Interferometry. *Remote Sens.* 2020, 12, 1211.
52. Huang, Q.; Wang, Y.; Luzi, G.; Crosetto, M.; Monserrat, O.; Jiang, J.; Zhao, H.; Ding, Y. Ground-Based Radar Interferometry for Monitoring the Dynamic Performance of a Multitrack Steel Truss High-Speed Railway Bridge. *Remote Sens.* 2020, 12, 2594.
53. Artese, S.; Nico, G. TLS and GB-RAR Measurements of Vibration Frequencies and Oscillation Amplitudes of Tall Structures: An Application to Wind Towers. *Appl. Sci.* 2020, 10, 2237.
54. Miccinesi, L.; Michelini, A.; Pieraccini, M. Blurring/Clutter Mitigation in Quarry Monitoring by Ground-Based Synthetic Aperture Radar. *IEEE Trans. Geosci. Remote Sens.* 2021.
55. Miccinesi, L.; Beni, A.; Pieraccini, M. Multi-Monostatic Interferometric Radar for Bridge Monitoring. *Electronics* 2021, 10, 247.